

# A biomimetic approach to evaluate mineralization of bioactive glass-loaded resin composites

Jiaojiao Yun <sup>a</sup>, Kwong-Hoi Tsui <sup>a,b</sup>, Zhiyong Fan <sup>b</sup>, Michael Burrow <sup>c</sup>, Jukka P. Matinlinna <sup>a</sup>, Yan Wang <sup>d</sup>, James K.H. Tsoi <sup>a,\*</sup>

<sup>a</sup> Dental Materials Science, Division of Applied Oral Sciences and Community Dental Care, Faculty of Dentistry, The University of Hong Kong, Hong Kong SAR, China

<sup>b</sup> Department of Electronic and Computer Engineering, Hong Kong University of Science and Technology, Hong Kong SAR, China

<sup>c</sup> Prosthodontics, Division of Restorative Dental Sciences, Faculty of Dentistry, The University of Hong Kong, Hong Kong SAR, China

<sup>d</sup> Department of Prosthodontics, Guanghua School of Stomatology, Hospital of Stomatology, Guangdong Key Laboratory of Stomatology, Sun Yat-sen University, China

## Abstract

**Purpose:** This study explores novel solutions other than standard SBF for biomimetic evaluations of mineralization particularly for resin composites containing bioactive glass (BAG).

**Methods:** Experimental UDMA/TEGDMA resin composites with 0.0, 1.9, 3.8 or 7.7 vol% of 45S5 BAG fillers were prepared. Besides simulated body fluid (SBF) as control, the specimens were immersed in three other solutions either with bicarbonate which are Hank's balanced salt solution (HBSS) and cell culture medium (MEM), or without bicarbonate which is a novel Simple HEPES-containing Artificial Remineralization Promotion (SHARP) solution, for 3, 7 and 14 days. These solutions were then analyzed by ICP-OES and pH, and the surfaces of the BAG composites were analyzed by SEM, XRD and FTIR.

**Results:** ICP-OES revealed Ca and P concentration continuously decrease, while Si concentration increases with time in the solutions other than SBF, which showed almost unchanged elemental concentration. Only SHARP solution is able to maintain a constant pH over the immersion time. SEM, together with XRD and FTIR, showed nano-sized octacalcium phosphate (OCP) nanospheres formation on 3.8 and 7.7 vol% BAG composites after 14 days immersion in HBSS (500–600 nm) and MEM (300–400 nm). SHARP solution enabled OCP formation after 3 days and then self-assembled into urchin-like carbonated hydroxyapatite (CHA) microspheres encompassed with nanorods of 100 nm width and 8 μm length after 14 days of immersion for 7.7 vol% BAG composites.

**Conclusion:** This study suggests SHARP solution can evaluate mineralization biomimetically whereas CHA microspheres can be formed on BAG-containing resin composites.

**Keywords:** Hydroxyapatite, Biomimetic, Mineralization, Bioactive glass, Resin composite

Received 14 July 2021, Accepted 4 November 2021, Available online 22 February 2022

## 1. Introduction

Bioactive glasses (BAG), first melt-derived in the late 1960s by Larry Hench, obtained good clinical results in dentistry, due to their properties of good bioactivity, when used to treat bone defects[1]. The composition of this bioactive glass was 45 wt% SiO<sub>2</sub>, 24.5 wt% Na<sub>2</sub>O, 24.5 wt% CaO, and 6 wt% P<sub>2</sub>O<sub>5</sub>, which was later termed as 45S5 or Bioglass®. Recently, various researchers have incorporated BAG into experimental[2–5] and commercial dental resin composite materials[6]. The release of calcium and phosphate ions was used as a means to assist with prevention of demineralization of dentine from an initial caries attack. Furthermore, BAG-containing resin compos-

ites can reduce bacterial penetration into marginal gaps due to their ability to increase local pH, precipitate apatite on the surface, or in this case within the gap[7]. In addition, a novel design of resin composite-based implant containing bioactive glass has successfully been used for many years[8,9]. The fiber-reinforced composite implants loaded with bioactive glass were supported to enhance biological bone repair and the formation of vascularized structures, in addition to providing improved antimicrobial properties for implants. Chemically speaking, this type of “bioactive” action is a mineralization reaction. At the beginning, a silica-rich layer with Si-OH groups forms on the surface by the exchange of Na<sup>+</sup> and Ca<sup>2+</sup> ions from the glass with surrounding H<sup>+</sup> ions, which increases surrounding pH. Then, Ca<sup>2+</sup> and PO<sub>4</sub><sup>4-</sup> from surrounding solution forms amorphous calcium phosphate (ACP, Ca<sub>x</sub>(PO<sub>4</sub>)<sub>y</sub>·nH<sub>2</sub>O)[10] on the surface, which is transformed into octacalcium phosphate (OCP, Ca<sub>8</sub>(HPO<sub>4</sub>)<sub>2</sub>(PO<sub>4</sub>)<sub>4</sub>·5H<sub>2</sub>O)[10] and finally evolves into nanocrystalline carbonated hydroxyapatite (CHA, Ca<sub>10-x</sub>(PO<sub>4</sub>)<sub>6-x</sub>(CO<sub>3</sub>)<sub>x</sub>(OH)<sub>2-x-2y</sub>(CO<sub>3</sub>)<sub>y</sub>) not hydroxyapatite (HA, Ca<sub>10</sub>(PO<sub>4</sub>)<sub>6</sub>(OH)<sub>2</sub>) in human body as bone or tooth enamel[11,12].

DOI: [https://doi.org/10.2186/jpr.JPR\\_D\\_21\\_00177](https://doi.org/10.2186/jpr.JPR_D_21_00177)

\*Corresponding author: James K.H. Tsoi, Dental Materials Science, Division of Applied Oral Sciences and Community Dental Care, Faculty of Dentistry, The University of Hong Kong, 34 Hospital Road, Sai Ying Pun, Hong Kong SAR, China.

E-mail address: [jkhtsoi@hku.hk](mailto:jkhtsoi@hku.hk)

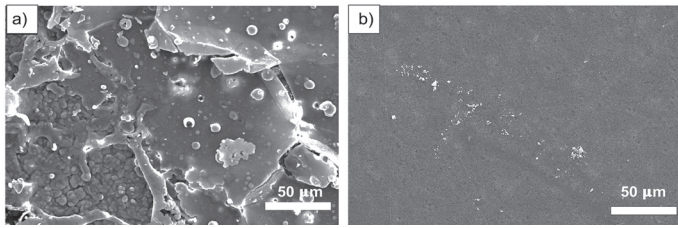


**Fig. 1.** SEM images of resin composites containing (a) 70 wt% BAG (Reproduced with permission[15]) and (b) 20 wt% BAG (7.7 vol%) after 7 days of immersion in SBF.

Simulated body fluid (SBF) with ionic concentrations similar to those of human blood plasma has been widely used for the assessment of so-called *in vitro* “bioactivity”. In Rehman’s study, the apatite crystals were found on 45S5 Bioglass® disks when immersed in SBF[13]. However, the statement of “bioactivity” has a contradiction to the experiment result that, e.g.  $\beta$ -TCP does not always lead to apatite formation in SBF despite showing extensive bonding to bone[14]. Therefore, the mimicry of bioactivity using SBF is still debatable. In addition, a previous study[15] showed the apatite could form on 70 wt% 45S5 BAG-loaded UDMA-based resin composites after 7 days immersion in SBF (Fig. 1a). In particular, as shown in Figure 1b, no apatite formation was observed on UDMA-based resin composites containing 20 wt% (7.7 vol%) 45S5 BAG after 7 days immersion in SBF. Lu et al. showed that using SBF and  $K_2HPO_4$  solution to evaluate *in vitro* bioactivity of bioactive materials was susceptible to testing solutions and conditions[16]. This suggested that SBF may not be a suitable medium for all kinds of bioactive composite materials, for example, in case of low content of BAG resin composite which has shown promising results in cell[17], animal[18] and clinical[19] studies but could not induce calcium phosphate-based mineralization in SBF.

Alternative immersion solutions have been proposed for the assessment of formation of calcium phosphate (CaP) on bioactive material. One study[20] used a cell culture medium, which was claimed to be easily prepared, when compared with a conventional SBF. In addition, cell culture medium was proposed to simulate an *in vivo* environment. It is worth noting that the cellular microenvironment plays a key role in cell proliferation and differentiation. Because differentiation of cells does not happen, and cells can eventually die under the condition of high pH level[21]. Other work demonstrated deposition of CaP as a coating on the substrate by simple immersion of specimens in Hank’s solution[22], while the study by Al-eesa et al., indicated that hydroxyapatite could form on BAG-resin adhesive when the specimen was exposed to an artificial saliva[23]. Furthermore, their research revealed that the release of Ca, P, and F to the surrounding solution was noticeable when the storage medium was acidic[5]. Thus, these studies have indicated that the different properties of various immersion solutions, such as the presence or absence of some ions that are necessary for apatite formation and the pH, could influence the formation of CaP. However, the morphology and structure of the formed calcium phosphate are still worth studying, which play an essential role on cellular behavior[24]. In addition, the research outlined above only studied the release of Ca, P, and F, with few data on the release of Si from BAG-loaded resin composites, which plays an important role in cells activity[25] and thus can enhance the bioactivity[26].

Due to release of various elements, the increase in BAG loading could lead to excessive water exchange between the bioactive glass and storage solution, which will result in the loss of desired physical and mechanical properties. In fact, one study has shown that the compressive and flexural strength of resin composite decreased significantly when 30 wt% BAG was added to resin composites[27], whereas another study has shown that increasing the BAG content up to 15 wt% did not affect the flexural strength and fracture toughness of the tested resin composites[28]. On the other hand, whilst a high content of ions or elemental release from the BAG could be beneficial for the remineralization of demineralized dentine, it may have the unwanted consequence of destroying cell viability at the same time. It was shown that increasing BAG content caused a proportional reduction of metabolic activity of human mesenchymal stromal cells due to the release of ions[29]. Therefore, to solve this potential problem, a low content of BAG might be useful in maintaining the ability to for (re)mineralization, without risking a change to the mechanical and physical properties and toxicity of a resin composite.

Given the inadequacy of storage in SBF to assess the CaP mineralization ability of resin composite containing low quantities of BAG, and the proposed procedure for preparing SBF solutions is long and tricky, a different mineralizing solution seems necessary. The aim of this study was to investigate the effects of  $Ca^{2+}$  and  $PO_3^{4-}$  containing solutions on the CaP formation of resin composites containing low quantities of BAG fillers (0.0, 1.9, 3.8, and 7.7 vol%). The traditional SBF solution was used as positive control. Two of them containing bicarbonate were Hank’s balanced salt solution (HBSS), and a cell culture medium (MEM). Furthermore, a Simple HEPES-containing Artificial Remineralization Promotion (SHARP) solution without bicarbonate was formulated and used in this study. The release of various elements (Ca, P, and Si), the changes in pH, and the ability of the experimental resin composites to form CaP will be explored.

## 2. Materials and Methods

### 2.1 Preparation of resin composites

Resin composite was prepared using a resin mixture of urethane dimethacrylate and triethylene glycol dimethacrylate (UDMA/TEGDMA=50:50 w/w) (Esstech, Inc., PA). The photoinitiators, including camphorquinone (CQ) and dimethylaminoethyl methacrylate (DMAEMA) (Esstech, Inc., PA), were added and mixed homogeneously into the resin mixture at 1 wt%. Control resin composite was prepared by mixing the resin matrix with 25 vol% (~65wt%) of commercial silanized dental glass filler (DF11,  $D_{50}=0.7\mu m$ , density 2.5-2.6 g/cm<sup>3</sup>, Cera Dynamics Ltd, England). DF11 contains 72 wt%  $SiO_2-Al_2O_3-B_2O_3$ , 25 wt% BaO, 2 wt% F, and 1 wt% unknown component, which is not mentioned in the composition. For the experimental composites, three quantities of the BAG fillers were used, namely, 1.9, 3.8 or 7.7 vol% of 45S5 bioactive glass (BAG,  $D_{50}=4\mu m$ , density 2.5-5.6 g/cm<sup>3</sup>, Schott® Vitryxx®, Germany). The different filler contents were loaded into the matrix resin and contributed to the total filler load with same dental glass filler up to 25 vol% (~65 wt%) as the control composite. All constituents were placed inside a glass beaker, which was covered with aluminum foil to protect the resin composites from ambient light, and then hand-mixed homogeneously with a spatula for 5 mins. The aluminum foil covered syringes were used to store well mixed resin composites and stored in fridge at 4°C. Each resin composite was placed into a Teflon mold (inner diameter=6.0 mm, thickness=1.0 mm), covered with a glass slide, then photo-cured using an LED curing light with an output of 1100 mW/cm<sup>2</sup> (Bluephase®

**Table 1.** The composition and its concentration (in mM) of SBF, HBSS, MEM and SHARP solution

Composition	SBF	HBSS	MEM	SHARP solution
CaCl <sub>2</sub>	3	1.26	1.80	1.5
KH <sub>2</sub> PO <sub>4</sub>	-	0.44	-	0.9
K <sub>2</sub> HPO <sub>4</sub>	1	-	-	-
NaH <sub>2</sub> PO <sub>4</sub>	-	-	1.01	-
Na <sub>2</sub> HPO <sub>4</sub>	-	0.34	-	-
KCl	3	5.37	5.33	50
NaCl	137	136.89	117.24	-
MgCl <sub>2</sub>	1.5	0.49	-	-
MgSO <sub>4</sub>	-	0.41	0.81	-
Na <sub>2</sub> SO <sub>4</sub>	0.5	-	-	-
NaHCO <sub>3</sub>	4	4.17	26	-
Tris	51	-	-	-
HEPES	-	-	-	20
pH	7.4	6.7-7.8	7.0-7.4	7.4

Style Curing Light, Ivoclar Vivadent, Lichtenstein) for 40s, and stored in a dry, dark environment at room temperature for 1 day before experiments.

## 2.2 Surface static water contact angles of resin composites

The static sessile drop contact angle was measured by dropping 5.0  $\mu$ L of deionized water on the surface of the as cured resin composites using an auto-pipette. Immediately after placing the drop on the surface, pictures of each drop were captured and analyzed using a goniometer approach[30,31]. Measurements were obtained in triplicate for each sample (n=4 per group).

## 2.3 The distribution of BAG fillers in resin composites

Since the commercial dental glass filler does not contain calcium, Ca elemental mapping using X-ray energy dispersive spectroscopy (EDX, SU1510, Hitachi, High-Technologies Corporation, Tokyo, Japan) was applied on EDX images (127 $\times$ 95  $\mu$ m<sup>2</sup>) at  $\times$ 1000 to analyze the distribution of BAG fillers in the experimental composites. The area ratios of BAG fillers to resin composites were assessed by using image analysis software (ImageJ, NIH, Bethesda, MD, USA). Three fields from each sample were analyzed by firstly subtracting the area ratios of the group without BAG fillers from the area ratios of all other 1.9 vol%, 3.8 vol%, and 7.7 vol% BAG loaded resin composites, and then averaging the results. The linear regression was conducted to analyze the relationship between the area ratio and contents of BAG fillers using Graphpad Prism 9.

## 2.4 Immersion of resin composites in different solutions

Five immersion solutions, including simulated body fluid (SBF), Hank's balanced salt solution (HBSS), cell culture media (MEM), a Simple HEPES-containing Artificial Remineralization Promotion (SHARP) solution, and deionized water (DI water), were used in this study (Table 1). The SBF with a composition of 137 mmol/L NaCl, 3 mmol/L KCl, 1.5 mmol/L MgCl<sub>2</sub>·6H<sub>2</sub>O, 1 mmol/L K<sub>2</sub>HPO<sub>4</sub>·3H<sub>2</sub>O, 3mmol/L CaCl<sub>2</sub>, 0.5mmol/L Na<sub>2</sub>SO<sub>4</sub>, 4 mmol/L NaHCO<sub>3</sub>, 51 mmol/L and pH of 7.4 was prepared carefully following formulations and protocols mentioned by Kokubo et al.[32]. HBSS (Gibco, Thermo Fisher Scientific, USA) consisted of 1.26 mmol/L CaCl<sub>2</sub>, 0.49 mmol/L MgCl<sub>2</sub>·6H<sub>2</sub>O, 0.41 mmol/L

MgSO<sub>4</sub>·7H<sub>2</sub>O, 5.37 mmol/L KCl, 0.44 mmol/L KH<sub>2</sub>PO<sub>4</sub>, 4.17 mmol/L NaHCO<sub>3</sub>, 136.89 mmol/L NaCl and 0.34 mmol/L Na<sub>2</sub>HPO<sub>4</sub> (pH range: 6.7-7.8). MEM was prepared by mixing Eagle's minimum essential medium with 10% fetal bovine serum (Gibco, Thermo Fisher Scientific, USA). SHARP solution used in this study was prepared by mixing 1.50 mmol/L CaCl<sub>2</sub>, 50.00 mmol/L KCl, 0.90 mmol/L KH<sub>2</sub>PO<sub>4</sub> and 20.00 mmol/L HEPES (pH 7.4). Each resin composite specimen (n=3) was stored in 5 mL of each solution in Corning® 15 mL polypropylene conical falcon centrifuge tubes. No solution change was performed during the immersion period. After 3, 7, and 14 days, all specimens (respectively named with suffix 3d, 7d, and 14d) were thoroughly rinsed with deionized water and dried at room temperature.

### 2.4.1 Elemental release analysis

In order to understand the reaction of BAG-loaded resin composites in different immersion solutions, the elemental releases of Ca, P, and Si as a function of immersion time were measured by inductively coupled plasma-optical emission spectrometry (ICP-OES) (Spectro Arcos, SPECTRO Analytical Instruments GmbH, Boschstr, Kleve, Germany). After 3, 7, and 14 days, 4mL of each storage solution were sucked into ICP-OES directly from falcon centrifuge tube of each group with a hyphenated autosampler (Cetac ASX 520, USA). Before measurement, the instrument was calibrated using calcium standard, phosphorous standard, and silicon standard solutions (Sigma-Aldrich, USA), which were diluted to prepare a set of diluted standards. The standard curves were obtained by plotting the intensity (counts) for each standard vs. its concentration in mg/L. The concentration of each unknown sample was calculated from the standard curves. The measurements were triplicated.

### 2.4.2 pH measurement

A pH meter (Oakton Ion 2700 Benchtop Meter, USA) with pH probe (Oakton wd-35805-04, USA) was calibrated before each measurement. Buffer with pH values of 4.01, 7.00 and 10.01 were used for the calibration. Then, the pH values of the different storage solutions were measured after 3, 7, and 14 days. The measurements were triplicated on each sample.

### 2.4.3 Surface characterization analysis

After 3, 7, and 14 days of immersion, samples were washed with deionized water and dried at room temperature before surface characterization analysis. The surface morphology of the specimens was analyzed by scanning electron microscopy (SEM) (SU1510, Hitachi, High-Technologies Corporation, Tokyo, Japan) with Platinum/palladium (Pt/Pd) sputter coating. ImageJ software was used to analyze the sizes of the formed calcium phosphate on the specimens. The chemical elements of the surface of samples were characterized by X-ray photoelectron spectroscopy (XPS) (Kratos Axis Ultra DLD) using monochromatic Al K $\alpha$  radiation operating at 150 watts, with a base pressure of 10<sup>-9</sup> Pa. Hybrid Image was used and data sets were acquired in parallel using a hemispherical mirror analyzer, with a microchannel plate and delay line detector. An X-ray diffractometer (XRD) (Rigaku SmartLab 9 kW, Japan) was used in conjunction with a copper x-ray source to scan the surface of specimens with a scanning step of 0.02°, scanning speed of 0.1 s/step, and a scanning range of 10-60°. The collected spectra were analyzed using JADE8 software (Materials Data Inc., JADE, Livermore, CA). The structural aspects of the calcium phosphate were determined by attenuated total reflectance-fourier transform infrared spectroscopy (ATR-FTIR)

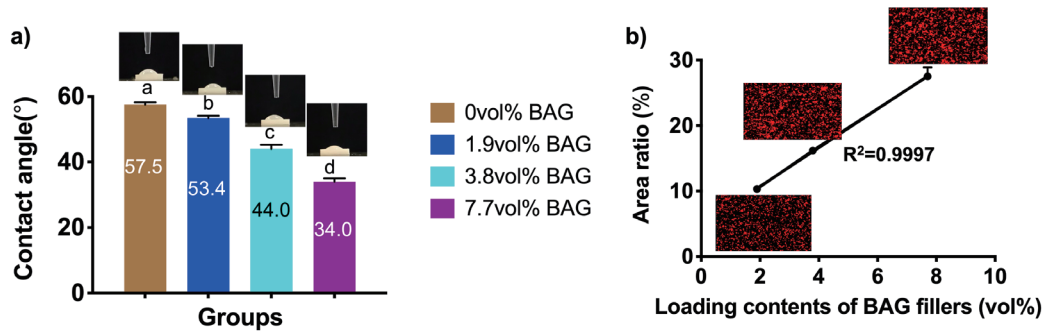


**Fig. 2.** (a) Static contact angles of water on the experimental composites and (b) area ratios of BAG fillers (via EDX of Ca element) to different BAG vol% of resin composites. (Different small letters indicate significant differences between groups)

(PerkinElmer FT-IR Spectrometer Spectrum Two, USA). Spectra were obtained in the wavenumber range from 400<sup>-1</sup> to 1600 cm<sup>-1</sup> with a resolution of 2 cm<sup>-1</sup> and scan times of 64.

### 2.5 Statistical analysis

Data were statistically analyzed by SPSS (V13, Chicago, IL, USA). After checking the data normality and homogeneity of variance, one-way ANOVA with a Bonferroni *post hoc* test analyzed the difference among different groups. *P* < 0.05 was considered to be statistically significant.

## 3. Results

### 3.1 Surface static water contact angles

The contact angles of water on the resin composites are shown in **Figure 2a**. The results showed that a decrease in contact angle was associated with a significant increase of BAG contents (*p* < 0.05). It indicated that the resin composite containing a higher amount of BAG showed an increase in the hydrophilic properties of the surface. The composite containing 7.7 vol% BAG showed the greatest hydrophilicity as shown by the lowest contact angle (34.0°), while the control group without BAG filler had the greatest contact angle of 57.5°.

### 3.2 The distribution of BAG fillers in resin composites

The distribution of BAG fillers in resin composites was determined by using elemental mapping for Ca. As shown in **Figure 2b**, BAG fillers were evenly distributed throughout the experimental resin composite, while the area ratio of BAG to resin composites was proportional to the BAG content (*R*<sup>2</sup>=0.9997), such that:

$$\text{Ca area ratio} = 2.955 \times \text{BAG vol\%} + 4.799$$

The 1.9 vol% BAG-filled composite had the lowest area ratio (10.3%), while composite containing 7.7 vol% BAG showed the highest area ratio (27.5%) among all groups.

### 3.3 Elemental release

The cumulative Ca and P releases are shown in **Figure 3**. The graphs showed that the concentration of Ca and P in the immersion solutions decreased with time for HBSS, MEM, and SHARP solution.

This was especially the case for the composites containing 3.8 and 7.7 vol% BAG. In DI water and SBF, no obvious change of Ca and P concentration was observed. All resin composites released Si into the immersion solutions except for SBF, which showing unchanged Si concentration. Furthermore, the release of Si was more evident for the higher BAG loading and DI water.

### 3.4 pH changes

pH results (**Fig. 4**) showed that the pH of DI water, SBF, HBSS, and MEM increased with immersion time regardless of the amount of BAG. A noticeable pH increase was observed with an increase of BAG loading when stored in DI water. The BAG loading did not seem to have a significant effect on pH change in HBSS and MEM. In contrast, the pH of SHARP solution remained constant at 7.4 over the 14 days of the experiment.

### 3.5 Surface characterization

The surface morphology of the resin composites after 14 days immersion in the different solutions is shown in **Figure 5**. There was no CaP formation on any of the resin composites stored in DI water and SBF. The control and 1.9 vol% BAG-loaded composite showed smooth surfaces no matter stored in any of the immersion solutions. A tightly packed CaP layer was mainly found on those composites containing 3.8 and 7.7 vol% BAG when immersed in HBSS or MEM. The greater the BAG content, the denser was the CaP layer on the surface. Some single and clustered spherical-shaped particles about 500-600 nm in diameter were observed on the surface of the specimens immersed in HBSS, while the size of particles on specimens in MEM was 300-400 nm. When immersed in the SHARP solution, microspheres self-assembled by nano-sized rods with a width of 100 nm and a length of 8 μm were found only on the 7.7 vol% BAG composite.

In order to explore the changes in surface morphology with time, SEM images of 7.7 vol% BAG-loaded composites immersing in different solutions over time are shown in **Figure 6**. There was no CaP formation on the specimens after immersion in DI water and SBF over time. Newly formed CaP layer composed of packed spherical particles was found after a relatively short immersion period in HBSS and MEM (3 and 7 days). After 14 days immersion, the layer became denser. However, the particle size of calcium phosphate remained unchanged. In contrast, single nanorods with the width of 100 nm

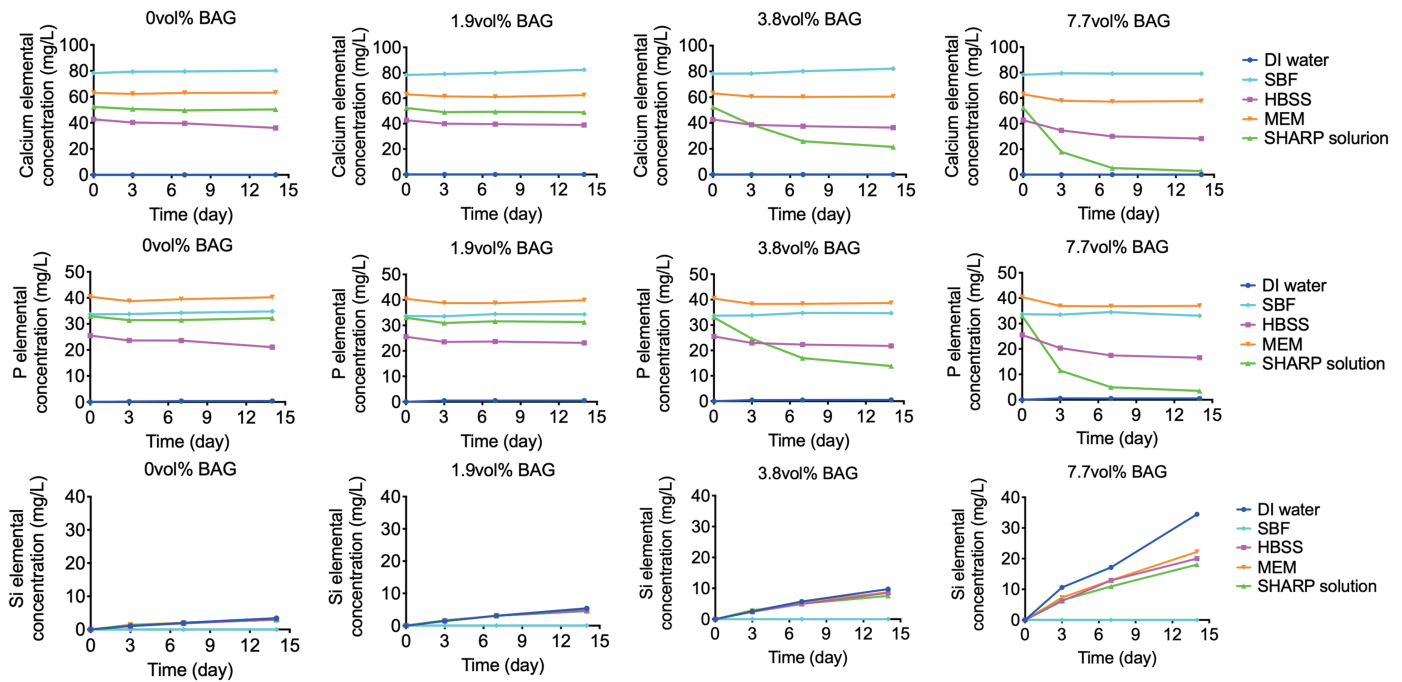


**Fig. 3.** Changes of Ca, P, and Si elemental concentration in DI water, SBF, HBSS, MEM, and SHARP solution as a function of immersion time.

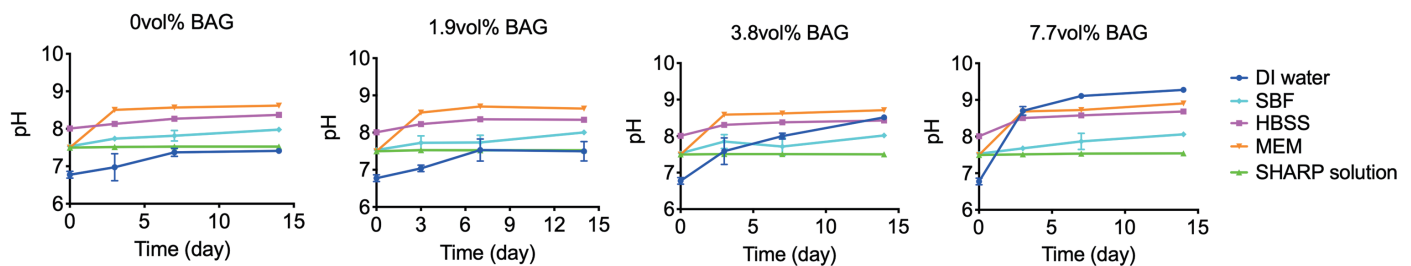


**Fig. 4.** pH changes of DI water, SBF, HBSS, MEM, and SHARP solution as a function of immersion time.

and the length about 0.8  $\mu\text{m}$  were found on the resin composites after 3 days of immersion in SHARP solution. The urchin-like microspheres became visibly larger as the immersion time in SHARP solution increased.

XPS measurements were performed to gain an insight into the elemental composition and its atomic concentration in CaP coating on resin composites (**Fig. 7**). Peak lines corresponding to Ca2p (347.4 eV) and P2p (133.0 eV) were clearly present on resin composites after 14 days of immersion in HBSS (3.8 vol% and 7.7 vol% BAG), SHARP solution (7.7 vol% BAG), and MEM (7.7 vol% BAG), which confirmed the formation of calcium phosphate. The atomic concentrations of calcium (Ca), phosphorous (P), oxygen (O), and Ca/P atomic ratios of the as-deposited Ca/P coatings were reported in **Table 2**. The atomic concentrations of Ca and P on 7.7 vol% BAG-resin composite in SHARP solution were 11.54% and 8.02%, respectively, which were the highest among all groups, and corresponding to atomic Ca/P ratios 1.44, i.e. a carbonated-containing hydroxyapatite[33]. For the 3.8 vol% BAG-resin composites in HBSS, and 7.7 vol% BAG-resin composites in HBSS and MEM, the atomic Ca/P ratios were respectively 1.18,

1.31, and 1.39, representing OCP or  $\alpha/\beta$ -tricalcium phosphates[33,34].

XRD was used to better identify the phase of calcium phosphate formed on the composite surfaces. As can be seen in **Figure 8a**, the XRD spectra of the calcium phosphate formed on resin composites stored in SHARP solution showed specific peaks at  $2\theta = 25.9^\circ, 28.1^\circ, 31.7^\circ, 32.9^\circ, 34.0^\circ, 46.7^\circ, 49.5^\circ, \text{ and } 53.2^\circ$ , which were assigned to the (002), (102), (211), (300), (202), (222), (213), and (004) planes of HA, respectively, according to ICDD PDF card number 09-0432. After immersion in HBSS and MEM, the primary phase of calcium phosphate showing specific peaks at  $2\theta = 24.4^\circ$  and  $29.3^\circ$ , was identified as (220) and (-312) planes of octacalcium phosphate (OCP), when compared with ICDD PDF card number 44-0778. Furthermore, no specific peak was found in spectra of 7.7 vol% BAG group after 3 days immersion (**Fig. 9a**), except for specimens stored in SHARP solution, which showed (220) planes at  $24.4^\circ$ . This indicates that calcium phosphate crystallized from OCP to HA well over time.

Additional FTIR spectra were shown in **Figures 8b and 9b**. The most intense bands observed at  $558\text{ cm}^{-1}$  and  $1000\text{--}1100\text{ cm}^{-1}$ , which

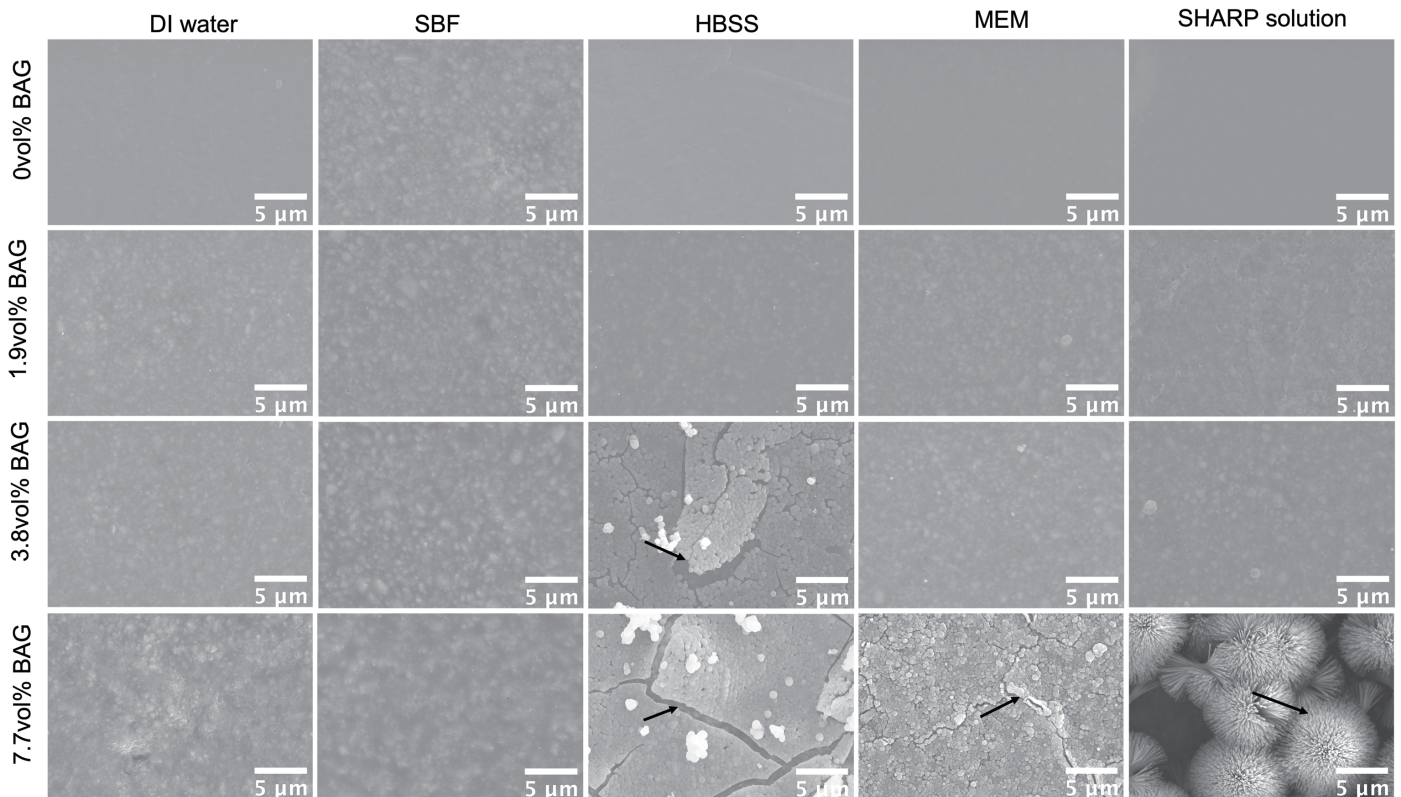


**Fig. 5.** Representative SEM images of resin composites containing different BAG contents after 14 days of immersion in DI water, SBF, HBSS, MEM, and SHARP solution, with arrows showing a tightly packed CaP layer composed of nano-sized spheres in HBSS (500–600 nm) and MEM (300–400 nm), and micro-sized urchin-like spheres of CaP in SHARP solution with a width of 100 nm and a length of 8 μm.

correspond to  $\nu_4$  and  $\nu_3$  bands of P–O stretching mode, indicated the presence of  $\text{PO}_4^{3-}$  group. Furthermore, characteristic peaks at  $875\text{ cm}^{-1}$  and  $959\text{ cm}^{-1}$  were found after 14 days immersion in HBSS for 3.8 and 7.7 vol% BAG-resin composites, and 14 days immersion in MEM for the 7.7 vol% BAG-resin composites. This indicated the presence of  $\text{HPO}_4^{2-}$  in the crystal. In contrast, after 14 days immersion of 7.7 vol% BAG-resin composites in SHARP solution, the bands detected at  $1460\text{ cm}^{-1}$ ,  $1420\text{ cm}^{-1}$ , as shown in the zooming patterns, and peaks at  $875\text{ cm}^{-1}$  indicated the presence of the  $\text{CO}_3^{2-}$  group of B-type carbonated apatite, where  $\text{PO}_4^{3-}$  groups were substituted by  $\text{CO}_3^{2-}$ . Additional peaks at  $603\text{ cm}^{-1}$  and  $1095\text{ cm}^{-1}$  were attributed to  $\nu_4$  and  $\nu_3$  stretching  $\text{PO}_4^{3-}$  vibration respectively. **Figure 9b** also showed the presence of those specific peaks even after a relatively short immersion period (3 and 7 days) for resin composites containing high contents of BAG (7.7 vol% BAG). In addition,  $\text{CO}_3^{2-}$  group of B-type carbonated apatite was also present in spectra of resin composites after 7 days of immersion in SHARP solution.

## 4. Discussion

### 4.1 Elemental release and pH change

Technically speaking, Al-eesa et al.[23] have used a similar sensitive analytical technique (ICP-OES) that this study also used, which indeed cannot distinguish whether the analyte being sampled is in ion or small particle form. Hence, we are conservative and cautiously in mentioning “elemental release” not the “ion release” throughout the current study. In this study, low content BAG-resin composites

have shown various behaviors of elemental release and pH change when immersed in different solutions over 14 days (**Figs. 3 and 4**). In DI water, SBF, HBSS, and MEM, pH increased with time. This indicated that the Ca in the BAG fillers was exchanged with surrounding  $\text{H}^+$  resulting in an increase of pH of storage solution. Notably, the increase of pH was slight in the Tris-buffered SBF, and no obvious change of elemental concentration was found due to the buffering effect of the Tris[5]. Furthermore, the evaluated pH in DI water was more evident for the composites containing greatest loading of BAG. This finding could be explained by the fact that the higher BAG-loading created an increase in the surface hydrophilicity (**Fig. 2a**) that was believed to improve the water sorption at the surface and into the body of the composite. This would accelerate the exchange of ions from the BAG fillers with surrounding  $\text{H}^+$ . Similarly, Mehdawi et al. study showed that the early water sorption into resin composites was proportional to the BAG content, which induced ion release for remineralization[35]. On the contrary, when stored in SHARP solution, the pH of the immersion solution remained unchanged due to the presence of HEPES.

### 4.2 Calcium phosphate (CaP) formation in the different immersion solutions

In the case of DI water and SBF, no distinctive precipitation layer was found even on 7.7 vol% BAG-loaded composite (**Fig. 5**). However, using another solution (e.g. Tris buffer) without  $\text{Ca}^{2+}$  and  $\text{PO}_4^{4-}$ , Al-eesa et al. have shown apatite deposition on the BAG-composites after only six hours immersion[23]. It should be noticed that their

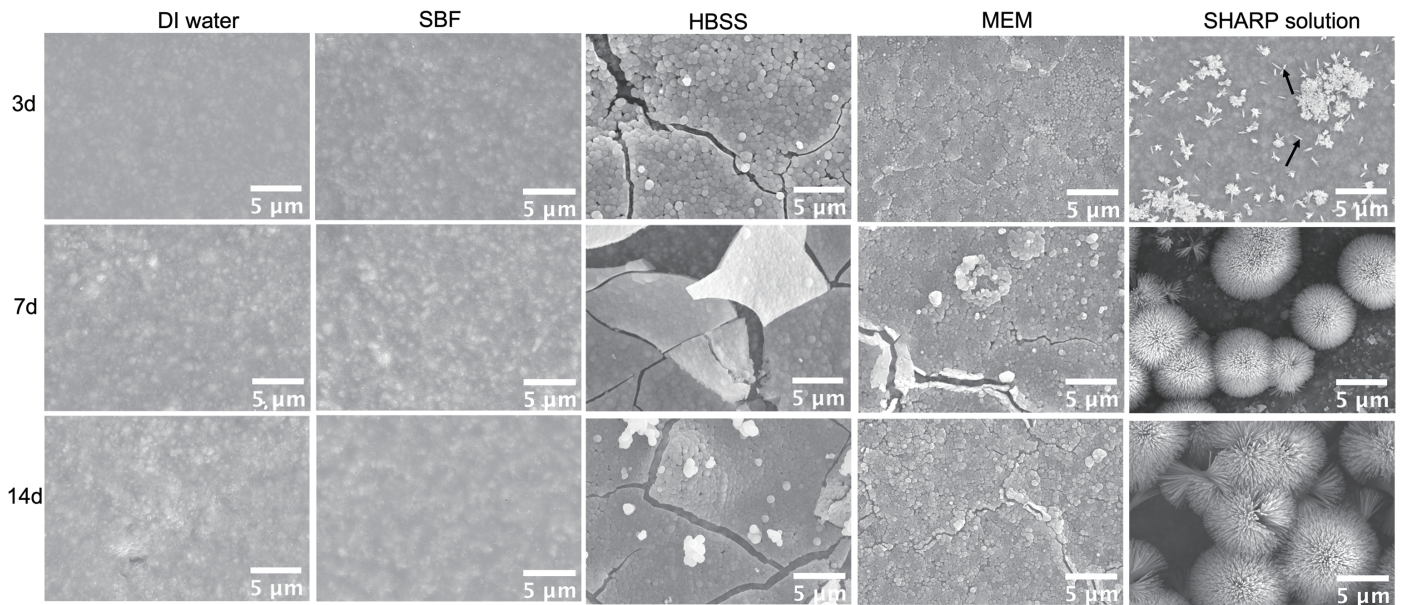


**Fig. 6.** Representative SEM images of 7.7 vol% BAG-loaded resin composites after immersion in DI water, SBF, HBSS, MEM, and SHARP solution for 3, 7, and 14 days, with arrow showing nanorod.

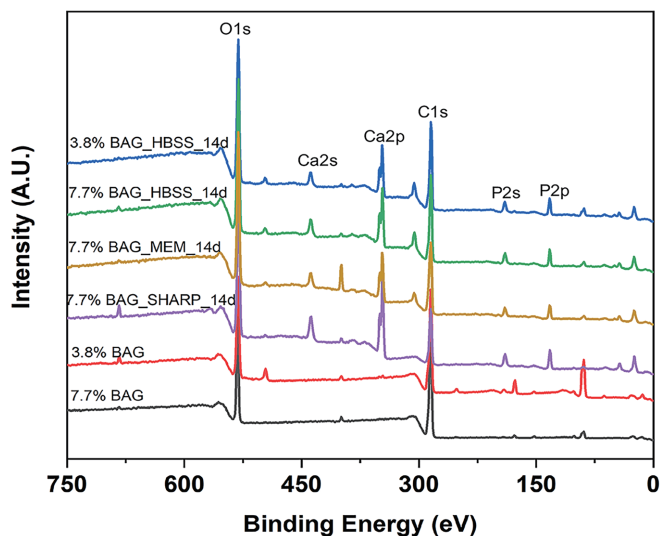


**Fig. 7.** XPS survey spectra of resin composites containing different BAG contents before and after 14 days immersion respectively in HBSS, MEM, and SHARP solution.

composites contained 80 wt% BAG as fillers, which was much higher than 0.0–7.7 vol% (0–20 wt%) used in the current study. Furthermore, apatite was also formed on 70 wt% 45S5 BAG-loaded resin composites[15]. Thus, the difference in the contents of BAG fillers may result in the variations in these two research outcomes. Furthermore, Al-eesa et al. also reported that there was a reactive layer existing on the surface of the BAG-resin disks after Tris buffer immersion due to the exchange of ions from the BAG fillers with the storage solution. Since the current study only showed the little release of calcium and phosphorus into DI water from the BAG-filled composites tested, there seems no supersaturation in the surrounding solution that might

**Table 2.** Atomic concentration of Ca, P, and O and Ca/P on resin composites containing different BAG contents after 14 days immersion in HBSS, MEM, and SHARP solution

Samples	% Atomic concentration			
	Ca2p	P2p	O1s	Atomic Ca/P
3.3 vol% BAG (without immersion)	0.00	0.00	23.35	-
7.8 vol% BAG (without immersion)	0.16	0.00	24.89	-
3.8 vol% BAG in HBSS	6.72	5.70	33.82	1.18
7.7 vol% BAG in HBSS	7.2	5.49	34.65	1.31
7.7 vol% BAG in MEM	5.58	4.01	32.11	1.39
7.7 vol% BAG in SHARP	11.54	8.02	39.89	1.44

lead to the formation of calcium phosphates. Furthermore, no obvious release of  $\text{Ca}^{2+}$  and  $\text{PO}_3^{4-}$  into SBF which cause no formed apatite on all resin composites. It can be inferred that calcium phosphate would form when the BAG content was increased as well as prolonging the immersion time[23]. The lack of bond between the BAG and the resin matrix would cause the mechanical alteration observed in resin materials. The previous study demonstrated that 30 wt% BAG loading led to a lowering of the compressive and flexural strength of the test resin composites[27]. This is why 7.7 vol% (~20 wt%) BAG was chosen as the highest filler loading in the current study. In addition, various studies[23,27] have used weight % instead of volume % for the filler content, which is indeed a tendency for an advertisement to “misdirect” the buyer, e.g. dentist, about “the higher the better” information[36]. Cautious should be taken in interpreting the information.

It can be seen from the **Figure 5** that when the resin composites were loaded with greater amounts of BAG there was greater formation of CaP after immersion in HBSS, MEM, and SHARP solution. In-

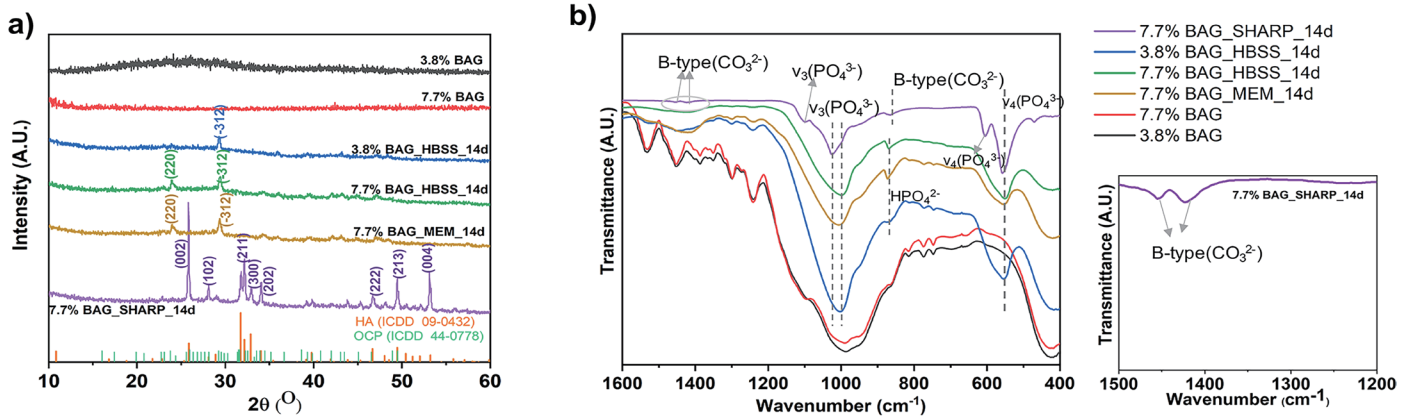


**Fig. 8.** (a) XRD patterns and (b) FTIR spectra of resin composites containing different BAG contents after 14 days of immersion in HBSS, MEM, and SHARP solution (The zooming patterns between 1500 and 1200  $\text{cm}^{-1}$  for 7.7 vol% BAG in SHARP solution was shown in the bottom right corner).

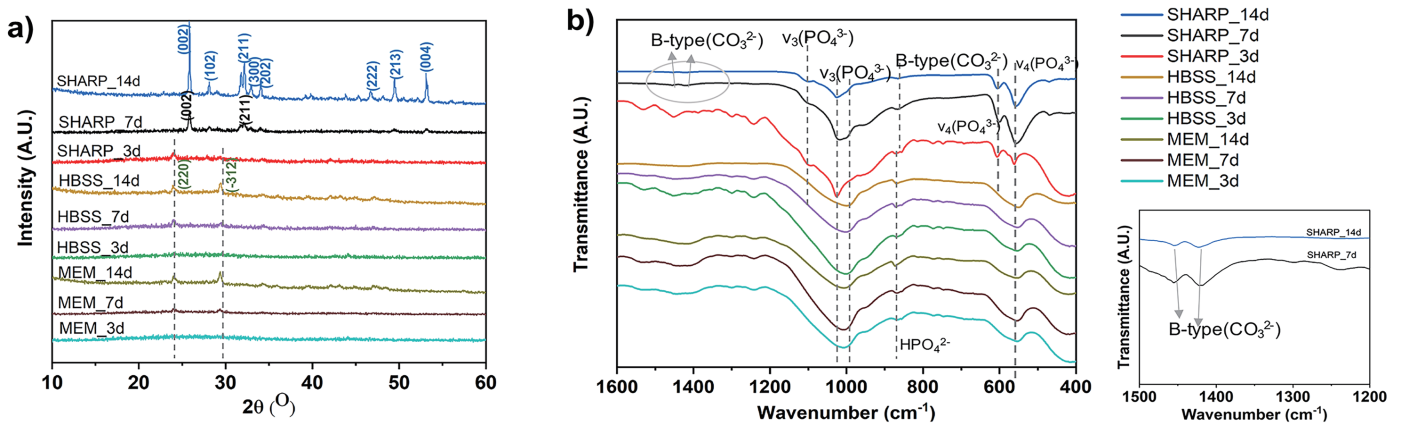


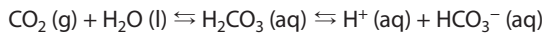
**Fig. 9.** (a) XRD patterns and (b) FTIR spectra of 7.7 vol% BAG-loaded resin composites after 3, 7, and 14 days of immersion in HBSS, MEM, and SHARP solution (The zooming patterns between 1500 and 1200  $\text{cm}^{-1}$  for 7.7 vol% BAG-composites after 7 and 14 days of immersion in SHARP solutions were shown in the bottom right corner). NB. Carbonated hydroxyapatite was observed only after 7 and 14 days of SHARP solution storage.

deed, the greater area of BAG fillers on the composite surface could provide more nucleation sites to promote the growth of calcium phosphate crystals (Fig. 2b). This is consistent with Al-eesa et al. study which has demonstrated that apatite was found on the surface with a higher Ca content due to the concentration gradient[23]. This can be explained by the increase of pH in surrounding solutions at the initial stage, which was more evident for higher BAG contents (Fig. 4). The ionic activity and the supersaturation of the solution in the region near the surface of resin composites increased. As a result, a calcium phosphate nucleated on the resin composites. Furthermore, more calcium phosphate formed as the immersion time increased (Fig. 6). As for immersion in HBSS and MEM, a homogeneous crystal layer was produced on 7.7 vol% BAG-resin composites even after a relatively short immersion time (3 day) and became denser without obvious changes of particle sizes. On the contrary, single nanorods with short length of about 0.8  $\mu\text{m}$  were seen after immersion in SHARP solution at the beginning (3 day). With prolonged immersion time, these single nanorods self-assembled into two-dimensional crystals. As a result, urchin-like microspheres consisting of nanorods with a width of 100 nm and a length of 8  $\mu\text{m}$  were formed on the surface of resin composites.

In addition to the different morphologies, the compositions of calcium phosphate formed on resin composites in different immersion solutions could be distinguished. As shown in XPS spectra, peaks attributed to calcium and phosphate were present (Fig. 7). The binding energies of these peaks were consistent with the reported XPS binding energies for Ca2p and P2p in calcium phosphates[33,34]. In particular, the atomic Ca/P ratio of the CaP coating on 7.7 vol% BAG-resin composite immersed in SHARP solution for 14 days is 1.44, which was a carbonate containing hydroxyapatite[33], consistent with the current XRD and FTIR results. For the BAG-resin composites immersed in HBSS and MEM, the XPS results can only identify the deposited CaP as OCP or  $\alpha/\beta$ -TCPs[33,34]. Indeed, it is difficult to differentiate calcium phosphate phases based on XPS binding energies alone, since the binding energies for calcium and phosphorous elements do not shift significantly among different calcium phosphate compounds. Thus, the composition of CaP precipitates was analyzed using XRD and FTIR (Figs. 8 and 9), and finally confirmed that the calcium phosphate crystals on resin composites in HBSS and MEM were OCP, particularly showing specific peaks at the 875  $\text{cm}^{-1}$  and 959  $\text{cm}^{-1}$  assigned to the  $\text{HPO}_4^{2-}$  group in the FTIR spectra[22]. This group is present in OCP, but absent in HA[27]. XRD spectrum of 7.7 vol% BAG specimens stored in SHARP for 14days had the strongest

peak intensity for the (002) reflection at 25.9°, which was consistent with Frank et al.[37]. This implied that the c-axis preferred orientation of the deposited crystals was (002) plane, despite the standard pattern of HA (ICDD 09-0432) showing the strongest peak (211) at 31.7°. It is worth to notice that the Ca/P ratio reported by XPS is in atomic ratio, which is not the same with the reported Ca/P ratio of 1.67 which is in molar ratio. Furthermore, as shown in **Figure 9a**, the diffraction peaks were high and narrow after longer immersion time, implying that calcium phosphate crystallized well over time. However, the peak showed at 24.4° may indicate that the initial formed calcium phosphate was OCP after 3 days immersion in SHARP solution, which could crystallize into CHA as time prolonged to 7 or 14 days.

The above results showed that SHARP solution was a favorable medium for carbonated hydroxyapatite deposition on the experimental BAG-resin composites, which resembled to the biological apatite[38,39]. However, if the study required mineralization of OCP on the surfaces, HBSS and MEM would be usable. Theoretically, the difference in the composition of CaP was thought to be mainly due to the composition of immersion solutions. MEM and HBSS contains bicarbonate (HCO<sub>3</sub><sup>-</sup>), which can buffer atmospheric CO<sub>2</sub> via the following equation by Le Chatelier's Principle:



As seen in **Figure 4**, the measured pH was increased to near to 8.5 from the original 7.4 and 8.0 for MEM and HBSS, respectively. This indicated that there was a decrease of H<sup>+</sup> concentration in surrounding solutions and the equilibrium was shifting to the left, which led to the decrease of concentration of HCO<sub>3</sub><sup>-</sup> in surrounding solutions. Therefore, no CO<sub>3</sub><sup>2-</sup> would be incorporated into calcium phosphate when immersing resin composites in HBSS and MEM. On the contrary, in some biological experiments that used MEM and HBSS[40], a CO<sub>2</sub> incubator which could supply a higher concentration of CO<sub>2</sub> was required so as to let more CO<sub>2</sub> dissolve in the solutions. Thus, more carbonic acid was generated, and surrounding pH could be kept. Moreover, MEM used in this study contained several enzymes, such as alkaline phosphatase. Previous study suggested that this enzyme may slow down the formation of HA[41] and stabilize the minerals in the precursor phases, such as ACP or OCP. However, HEPES in SHARP solution could keep the pH stable at 7.4 as seen from **Figure 4**. At the initial stage, there should be an increase of pH due to the exchange of Ca<sup>2+</sup> or Na<sup>+</sup> from BAG with surrounding H<sup>+</sup>. When the atmospheric CO<sub>2</sub> was dissolved in the SHARP immersion solution, the equilibrium was shifting to the right generating H<sup>+</sup> and HCO<sub>3</sub><sup>-</sup> in surrounding solution. The H<sup>+</sup> was either neutralized with the increased OH<sup>-</sup> or buffered by HEPES. As a result, pH in surrounding solutions could be kept stable and more HCO<sub>3</sub><sup>-</sup> was generated, which allowed CO<sub>3</sub><sup>2-</sup> incorporated into mineralization process[42,43]. Nonetheless, there is a need for the future study in the specific mechanism of OCP and carbonate-containing HA formation in these solutions.

## 5. Conclusion

This study concluded the SBF maybe not suitable for biomimetic evaluations of mineralization particularly for resin composites containing low quantities of bioactive glass (BAG). The SHARP solution can induce the controlled growth of urchin-like CHA microspheres self-assembled by nanorods for BAG-containing resin composite over time. Other solutions (HBSS and MEM) can deposit nano-sized OCP particles on the resin composites only.

## Acknowledgements

This work was done in partial fulfilment of the requirements of the degree of Doctor of Philosophy for the first author at the Faculty of Dentistry, The University of Hong Kong. This research acknowledge the grant support from The Natural Science Foundation of Guangdong Province, China (No. 2019A 1515011842). The authors declare no competing financial interest.

## Conflicts of Interest

The authors have declared that no conflict of interest exists.

## References

- [1] Hench LL, Splinter RJ, Allen WC, Greenlee TK. Bonding mechanisms at the interface of ceramic prosthetic materials. *J Biomed Mater Res.* 1971;5:117–41. <https://doi.org/10.1002/jbm.820050611>
- [2] Brown ML, Davis HB, Tufekci E, Crowe JJ, Covell DA, Mitchell JC. Ion release from a novel orthodontic resin bonding agent for the reduction and/or prevention of white spot lesions. *Angle Orthod.* 2011;81:1014–20. <https://doi.org/10.2319/120710-708.1>, PMID:22007662
- [3] Davis HB, Gwinner F, Mitchell JC, Ferracane JL. Ion release from, and fluoride recharge of a composite with a fluoride-containing bioactive glass. *Dent Mater.* 2014;30:1187–94. <https://doi.org/10.1016/j.dental.2014.07.012>, PMID:25175342
- [4] Yang SY, Kwon JS, Kim KN, Kim KM. Enamel surface with pit and fissure sealant containing 45S5 bioactive glass. *J Dent Res.* 2016;95:550–7. <https://doi.org/10.1177/0022034515626116>, PMID:26767770
- [5] Al-eesa NA, Wong FSL, Johal A, Hill RG. Fluoride containing bioactive glass composite for orthodontic adhesives – ion release properties. *Dent Mater.* 2017;33:1324–9. <https://doi.org/10.1016/j.dental.2017.08.185>, PMID:29029848
- [6] Tiskaya M, Al-eesa NA, Wong FSL, Hill RG. Characterization of the bioactivity of two commercial composites. *Dent Mater.* 2019;35:1757–68. <https://doi.org/10.1016/j.dental.2019.10.004>, PMID:31699444
- [7] Khvostenko D, Hilton TJ, Ferracane JL, Mitchell JC, Kruzic JJ. Bioactive glass fillers reduce bacterial penetration into marginal gaps for composite restorations. *Dent Mater.* 2016;32:73–81. <https://doi.org/10.1016/j.dental.2015.10.007>, PMID:26621028
- [8] Zhang D, Leppäranta O, Munukka E, Ylänen H, Viljanen MK, Eerola E, et al. Antibacterial effects and dissolution behavior of six bioactive glasses. *J Biomed Mater Res A.* 2010;93:475–83. <https://doi.org/10.1002/jbm.a.32564>, PMID:19582832
- [9] Posti JP, Piitulainen JM, Hupa L, Fagerlund S, Frantzén J, Aitasalo KMJ, et al. A glass fiber-reinforced composite – bioactive glass cranioplasty implant: A case study of an early development stage implant removed due to a late infection. *J Mech Behav Biomed Mater.* 2016;55:191–200. <https://doi.org/10.1016/j.jmbbm.2015.10.030>, PMID:26594779
- [10] Dorozhkin SV. Calcium orthophosphates. *J Mater Sci.* 2007;42:1061–95. <https://doi.org/10.1007/s10853-006-1467-8>
- [11] Landi E, Celotti G, Logroscino G, Tampieri A. Carbonated hydroxyapatite as bone substitute. *J Eur Ceram Soc.* 2003;23:2931–7. [https://doi.org/10.1016/S0955-2219\(03\)00304-2](https://doi.org/10.1016/S0955-2219(03)00304-2)
- [12] Lotsari A, Rajasekharan AK, Halvarsson M, Andersson M. Transformation of amorphous calcium phosphate to bone-like apatite. *Nat Commun.* 2018;9:4170. <https://doi.org/10.1038/s41467-018-06570-x>, PMID:30302020
- [13] Rehman I, Knowles JC, Bonfield W. Analysis of in vitro reaction layers formed on Bioglass using thin-film X-ray diffraction and ATR-FTIR microspectroscopy. *J Biomed Mater Res.* 1998;41:162–6. [https://doi.org/10.1002/\(SICI\)1097-4636\(199807\)41:1<162::AID-JBM19>3.0.CO;2-P](https://doi.org/10.1002/(SICI)1097-4636(199807)41:1<162::AID-JBM19>3.0.CO;2-P), PMID:9641636
- [14] Kotani S, Fujita Y, Kitsugi T, Nakamura T, Yamamuro T, Ohtsuki C, et al. Bone bonding mechanism of ?-tricalcium phosphate. *J Biomed Mater Res.* 1991;25:1303–15. <https://doi.org/10.1002/jbm.820251010>, PMID:1812121
- [15] Firdausy MD. Evaluation of experimental bioactive glass resin composites. (Thesis) The University of Hong Kong 2015. [https://doi.org/10.5353/th\\_b5573064](https://doi.org/10.5353/th_b5573064)

- [16] Lu X, Kolzow J, Chen RR, Du J. Effect of solution condition on hydroxyapatite formation in evaluating bioactivity of B<sub>2</sub>O<sub>3</sub> containing 45S5 bioactive glasses. *Bioact Mater*. 2019;4:207–14. <https://doi.org/10.1016/j.bioactmat.2019.05.002>, PMID:31198889
- [17] López-García S, Pecci-Lloret MP, Pecci-Lloret MR, Oñate-Sánchez RE, García-Bernal D, Castelo-Baz P, et al. In Vitro Evaluation of the Biological Effects of ACTIVA Kids BioACTIVE Restorative, Ionolux, and Riva Light Cure on Human Dental Pulp Stem Cells. *Materials (Basel)*. 2019;12:3694. <https://doi.org/10.3390/ma12223694>, PMID:31717445
- [18] About ElReash A, Hamama H, Abdo W, Wu Q, Zaen El-Din A, Xiaoli X. Biocompatibility of new bioactive resin composite versus calcium silicate cements: an animal study. *BMC Oral Health*. 2019;19:194. <https://doi.org/10.1186/s12903-019-0887-1>, PMID:31438924
- [19] Tirapelli C, Panzeri H, Lara EHG, Soares RG, Peitl O, Zanotto ED. The effect of a novel crystallised bioactive glass-ceramic powder on dentine hypersensitivity: a long-term clinical study. *J Oral Rehabil*. 2011;38:253–62. <https://doi.org/10.1111/j.1365-2842.2010.02157.x>, PMID:20868428
- [20] Lee JTY, Leng Y, Chow KL, Ren F, Ge X, Wang K, et al. Cell culture medium as an alternative to conventional simulated body fluid. *Acta Biomater*. 2011;7:2615–22. <https://doi.org/10.1016/j.actbio.2011.02.034>, PMID:21356333
- [21] Lagadic-Gossmann D, Huc L, Lecureur V. Alterations of intracellular pH homeostasis in apoptosis: origins and roles. *Cell Death Differ*. 2004;11:953–61. <https://doi.org/10.1038/sj.cdd.4401466>, PMID:15195071
- [22] Roguska A, Pisarek M, Andrzejczuk M, Dolata M, Lewandowska M, Janik-Czachor M. Characterization of a calcium phosphate-TiO<sub>2</sub> nanotube composite layer for biomedical applications. *Mater Sci Eng C*. 2011;31:906–14. <https://doi.org/10.1016/j.msec.2011.02.009>
- [23] Al-eesa NA, Johal A, Hill RG, Wong FSL. Fluoride containing bioactive glass composite for orthodontic adhesives—apatite formation properties. *Dent Mater*. 2018;34:1127–33. <https://doi.org/10.1016/j.dental.2018.04.009>, PMID:29779628
- [24] Yang H, Zeng H, Hao L, Zhao N, Du C, Liao H, et al. Effects of hydroxyapatite microparticle morphology on bone mesenchymal stem cell behavior. *J Mater Chem B Mater Biol Med*. 2014;2:4703–10. <https://doi.org/10.1039/C4TB00424H>, PMID:32262282
- [25] Han P, Wu C, Xiao Y. The effect of silicate ions on proliferation, osteogenic differentiation and cell signalling pathways (WNT and SHH) of bone marrow stromal cells. *Biomater Sci*. 2013;1:379–92. <https://doi.org/10.1039/C2BM00108J>, PMID:32481903
- [26] Balas F, Pérez-Pariente J, Vallet-Regí M. *In vitro* bioactivity of silicon-substituted hydroxyapatites. *J Biomed Mater Res A*. 2003;66A:364–75. <https://doi.org/10.1002/jbm.a.10579>, PMID:12889007
- [27] Korkut E, Torlak E, Altunsoy M. Antimicrobial and mechanical properties of dental resin composite containing bioactive glass. *J Appl Biomater Funct Mater*. 2016;14:e296–301. <https://doi.org/10.5301/jabfm.5000271>, PMID:27149938
- [28] Khvostenko D, Mitchell JC, Hilton TJ, Ferracane JL, Kruzic JJ. Mechanical performance of novel bioactive glass containing dental restorative composites. *Dent Mater*. 2013;29:1139–48. <https://doi.org/10.1016/j.dental.2013.08.207>, PMID:24050766
- [29] Qazi TH, Hafeez S, Schmidt J, Duda GN, Boccaccini AR, Lippens E. Comparison of the effects of 45S5 and 1393 bioactive glass microparticles on hMSC behavior. *J Biomed Mater Res A*. 2017;105:2772–82. <https://doi.org/10.1002/jbm.a.36131>, PMID:28571113
- [30] Wang Z, Sa Y, Sauro S, Chen H, Xing W, Ma X, et al. Effect of desensitising toothpastes on dentinal tubule occlusion: A dentine permeability measurement and SEM in vitro study. *J Dent*. 2010;38:400–10. <https://doi.org/10.1016/j.jdent.2010.01.007>, PMID:20097250
- [31] Zhang Y, Sun D, Cheng J, Tsoi JKH, Chen J. Mechanical and biological properties of Ti–(0–25 wt%)Nb alloys for biomedical implants application. *Regen Biomater*. 2020;7:119–27. <https://doi.org/10.1093/rb/rbz042>, PMID:32153995
- [32] Kokubo T, Takadama H. How useful is SBF in predicting in vivo bone bioactivity? *Biomaterials*. 2006;27:2907–15. <https://doi.org/10.1016/j.biomaterials.2006.01.017>, PMID:16448693
- [33] Lu HB, Campbell CT, Graham DJ, Ratner BD. Surface characterization of hydroxyapatite and related calcium phosphates by XPS and TOF-SIMS. *Anal Chem*. 2000;72:2886–94. <https://doi.org/10.1021/ac990812h>, PMID:10905323
- [34] Chusuei CC, Goodman DW, Van Stipdonk MJ, Justes DR, Schweikert EA. Calcium phosphate phase identification using XPS and time-of-flight cluster SIMS. *Anal Chem*. 1999;71:149–53. <https://doi.org/10.1021/ac9806963>, <https://doi.org/10.1021/Ac9806963>, PMID:21662937
- [35] Mehdawi IM, Pratten J, Spratt DA, Knowles JC, Young AM. High strength re-mineralizing, antibacterial dental composites with reactive calcium phosphates. *Dent Mater*. 2013;29:473–84. <https://doi.org/10.1016/j.dental.2013.01.010>, PMID:23434447
- [36] Darvell BW. Chapter 6 - Resin Restorative Materials. In: Darvell BW, editor. *Materials Science for Dentistry (Tenth Edition)*: Woodhead Publishing; 2018, p. 143–91.
- [37] Müller FA, Müller L, Caillard D, Conforto E. Preferred growth orientation of biomimetic apatite crystals. *J Cryst Growth*. 2007;304:464–71. <https://doi.org/10.1016/j.jcrysgro.2007.03.014>
- [38] Pan H, Darvell BW. Effect of carbonate on hydroxyapatite solubility. *Cryst Growth Des*. 2010;10:845–50. <https://doi.org/10.1021/cg901199h>
- [39] Liu Q, Huang S, Matinlinna JP, Chen Z, Pan H. Insight into biological apatite: physicochemical properties and preparation approaches. *BioMed Res Int*. 2013;2013:1–13. <https://doi.org/10.1155/2013/929748>, PMID:24078928
- [40] Han A, Ding H, Tsoi JKH, Imazato S, Matinlinna JP, Chen Z. Prolonged UV-C irradiation is a double-edged sword on the zirconia surface. *ACS Omega*. 2020;5:5126–33. <https://doi.org/10.1021/acsomega.9b04123>, PMID:32201799
- [41] Yun J, Wu J, Aparicio C, Tsoi JK, Wang Y, Fok A. Enzyme-mediated mineralization of TiO<sub>2</sub> nanotubes subjected to different heat treatments. *Cryst Growth Des*. 2019;19:7112–21. <https://doi.org/10.1021/acs.cgd.9b00966>
- [42] Uskoković V. X-ray photoelectron and ion scattering spectroscopic surface analyses of amorphous and crystalline calcium phosphate nanoparticles with different chemical histories. *Phys Chem Chem Phys*. 2020;22:5531–47. <https://doi.org/10.1039/C9CP06529F>, PMID:32123882
- [43] Barralet J, Best S, Bonfield W. Carbonate substitution in precipitated hydroxyapatite: an investigation into the effects of reaction temperature and bicarbonate ion concentration. *J Biomed Mater Res*. 1998;41:79–86. [https://doi.org/10.1002/\(SICI\)1097-4636\(199807\)41:1<79::AID-JBM10>3.0.CO;2-C](https://doi.org/10.1002/(SICI)1097-4636(199807)41:1<79::AID-JBM10>3.0.CO;2-C), PMID:9641627



This is an open-access article distributed under the terms of Creative Commons Attribution-NonCommercial License 4.0 (CC BY-NC 4.0), which allows users to distribute and copy the material in any format as long as credit is given to the Japan Prosthodontic Society. It should be noted however, that the material cannot be used for commercial purposes.